

Ab Initio Study of Interfacial Structure Transformation of Amorphous Carbon Catalyzed by Ti, Cr, and W Transition Layers

Xiaowei Li,^{*,†,‡,§} Lei Li,[†] Dong Zhang,[†] and Aiying Wang^{*,†}

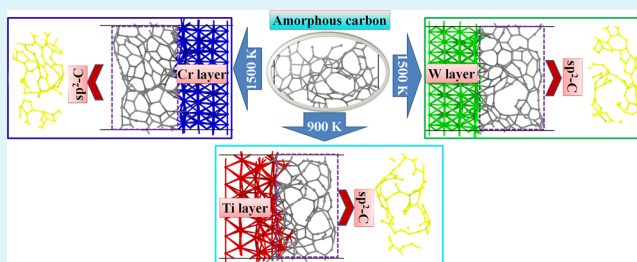
[†]Key Laboratory of Marine Materials and Related Technologies, Key Laboratory of Marine Materials and Protective Technologies of Zhejiang Province, Ningbo Institute of Materials Technology and Engineering, Chinese Academy of Sciences, Ningbo 315201, P.R. China

[‡]Computational Science Center, Korea Institute of Science and Technology, Seoul 136-791, Republic of Korea

Supporting Information

ABSTRACT: Amorphous carbon (a-C) films composited with transition layers exhibit the desirable improvement of adhesion strength between films and substrate, but the further understanding on the interfacial structure transformation of a-C structure induced by transition layers is still lacked. In this paper, using ab initio calculations, we comparatively studied the interfacial structure between Ti, Cr, or W transition layers and a-C film from the atomic scale, and demonstrated that the addition of Ti, Cr, or W catalyzed the graphitic transformation of a-C structure at different levels, which provided the theoretical guidance for designing a multilayer nanocomposite film for renewed application.

KEYWORDS: graphitic transformation, interfacial structure, transition layer, amorphous carbon, ab initio calculation



Amorphous carbon (a-C) film has attracted much attention in the past few years because of its superior mechanical and tribological properties, which is a strong candidate as protective coating in the fields of cutting tools, automobile, and so on.^{1–3} Especially, the controllable band gap of a-C film, originating from the modulation of sp³/sp² hybridized structure, generates the excellent optical properties, suggesting the potential optoelectronics applications, such as proton exchange membrane fuel cell.^{4–7} But the films are frequently prone to failure from the coated surface because of the existing poor film–substrate interfacial adhesion, especially on blank metal substrate.

Introducing a transition layer into a-C films has been proved to be an effective method to enhance the adhesion strength between the a-C and substrate,^{8,9} but it also catalyzes the special interfacial structure transformation.¹⁰ For example, Chen et al.⁸ reported that the addition of a Cr–C layer dramatically enhanced the adhesion of films to substrate, obtaining the critical load exceeding 80 N. Li et al.⁹ found that the ultrathin Cr/Al and Ti/Al dual interlayers offered the improved adhesion for diamond films and were also effective in suppressing the formation of graphitization structure on steel surface. However, Lee¹⁰ deposited the carbon films on different metal buffer layers at 700 °C, and revealed that carbon-nanoparticle films were produced with the Cr and W buffer layers, whereas the carbon-nanotube films were generated with the Ti and Ta buffer layers. Nevertheless, the effect of metal transition layers on the deposited a-C films from the atomic scale is still not fully understood yet. Especially, recent studies inspired that the graphene with high quality could be obtained

from a-C films by Ni or Cu-induced catalyzed effect under optimal temperature.^{11,12} Therefore, exploring the interfacial catalysis to a-C films induced by the metal transition layer and its temperature dependence are essential to account for the structural property evolution in experiment¹⁰ and optimize the conditions for functionalized carbon structure.

In the present work, we carried out the ab initio calculations to comparatively study the interfacial structure evolution between the a-C and different metal transition layers under different temperatures. The widely used Ti, Cr, and W metals were chosen as the transition layers separately for comparison. Figure 1a shows the models for a-C structure with different metal substrates (named as a-C@Me). Ti0001, Cr011, and W011 with four layers were chosen as the surface, which were composed of 72, 80, and 80 atoms, respectively; the used a-C film containing 116 carbon atoms and box size of 15.04 × 8.51 × 9 Å³ was obtained from ab initio molecular dynamics (AIMD) simulation by liquid quenching method,¹³ in which the original sp³ and sp² fractions were 23% and 60% separately. For each model, the corresponded average lattice mismatch between Ti, Cr, or W and a-C models were less than 2.5%. A vacuum of 15 Å was employed in the direction perpendicular to the surface to avoid spurious interactions across the periodic boundaries. Initial position between metal and a-C was 2 Å. Atoms in the bottom layer of the metal substrate were fixed to mimic the semi-infinite large surface.

Received: August 14, 2017

Accepted: November 14, 2017

Published: November 14, 2017

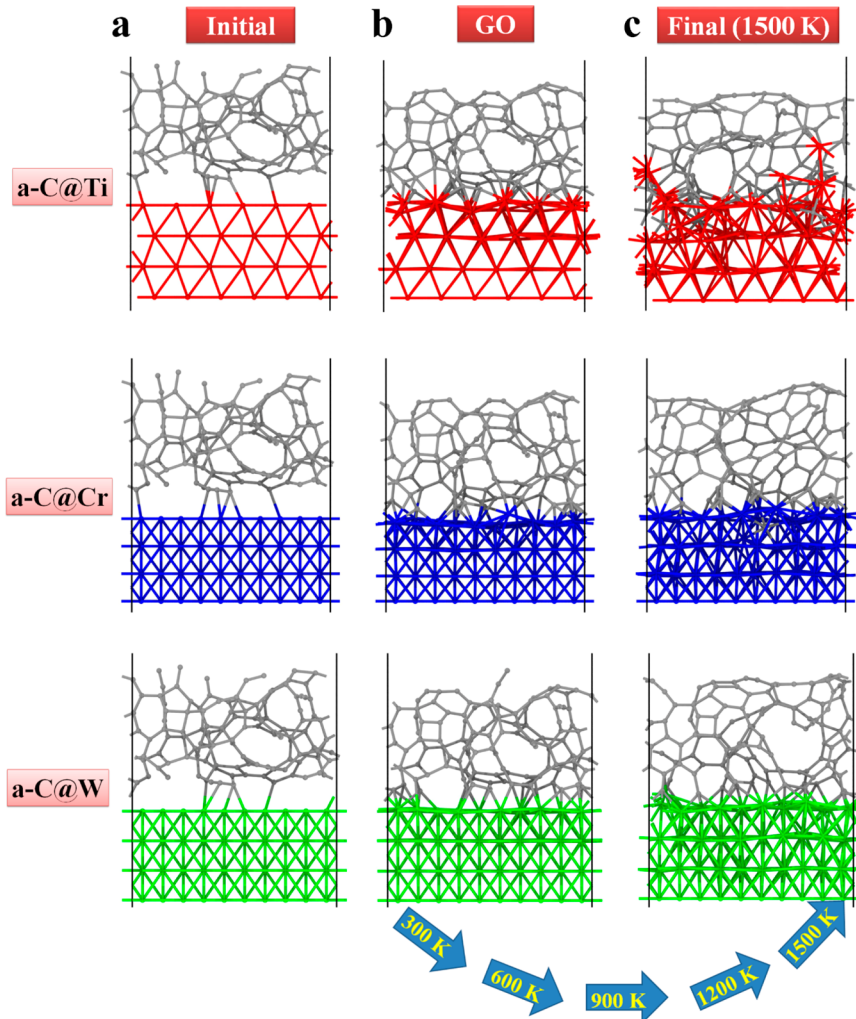


Figure 1. (a) Initial, (b) GO, and (c) final configurations of a-C@Ti, a-C@Cr, and a-C@W systems based on the stepwise temperature increase from 300, 600, 900, 1200 to 1500 K in AIMD simulations. The C, Ti, Cr, and W are shown in gray, red, blue, and green colors, respectively.

All calculations were performed by VASP software^{14,15} with a cutoff energy of 500 eV and a generalized gradient approximation with the Perdew–Burke–Ernzerhof parametrization.¹⁶ A two-step process composed of geometric optimization (GO) and AIMD simulation was used.¹³ During the GO process, a full relaxation of the atomic positions based on conjugated gradient¹⁷ was repeated to obtain the stable interface structures until the Hellmann–Feynman force on each atom was below 0.01 eV/Å, and the self-consistent loop was created using an energy convergence criterion of 1×10^{-4} eV. Then the system was relaxed by AIMD simulation at the stepwise increased temperature¹⁸ from 300 to 600, 900, 1200, and 1500 K (2 ps for each given temperature) using NVT ensemble with a Nose thermostat for temperature-control. Periodic boundary condition was employed along all directions. The Γ -only k-point was used to sample the Brillouin zone, and a MD time step of 1 fs was used. The energy change in Figure S1 showed that a relative stable state could be achieved for each case during the thermostatic process.

Before characterizing the structural evolution of a-C@Me systems, the cutoff radius values, R_{cut} , for C–C, C–Ti, C–W, C–Cr, Ti–Ti, W–W, and Cr–Cr were defined first by radial distribution functions (RDF) to evaluate whether they bond with each other or not. The RDF, $g(r)$, is proportional to the

density of atoms at a distance r from another atom, which is a very important parameter for structural characterization of amorphous materials, and it is computed by the formula

$$g(r) = \frac{dN}{\rho 4\pi r^2 dr} \quad (1)$$

where ρ is the average density of system, dN is the number of atoms from r to $r + dr$. Table 1 shows the cutoff radius for each case, which have been defined by previous work.¹⁹

Table 1. Cutoff Radius for C–C, C–Ti, C–W, C–Cr, Ti–Ti, W–W, and Cr–Cr Interactions

	C–C	C–Ti	Ti–Ti	C–Cr	Cr–Cr	C–W	W–W
R_{cut} (Å)	1.85	2.56	3.51	2.50	3.24	2.52	3.36

Figure 1 shows the initial, GO and final configurations at 1500 K of a-C@Ti, a-C@Cr, and a-C@W systems. After GO for initial a-C@Ti, a-C@Cr and a-C@W systems (Figure 1b), Ti, Cr, or W atoms could stabilize the dangling C atoms in the a-C layer; the distance between metal and a-C film decreases compared to the original 2 Å, and the obvious interactions between the C and Ti, Cr or W atoms can be observed as well; the sp³-C fraction for each case is 16.4, 16.4, and 16.4 at. %

separately, and the $\text{sp}^2\text{-C}$ fraction is 59.5, 59.5, and 58.6 at. %, respectively. After 10 ps AIMD simulation with stepwise temperature increase, the final configurations presented in Figure 1c show that in the a-C@Ti system, a few C atoms enter into the Ti layer, but the sharp interface is still observed in both a-C@Cr and a-C@W cases. Furthermore, the carbon roll structure is formed from a-C for each case, which agrees well with the previous experiment study,¹⁰ but the obvious holelike defect is generated in a-C@Ti and a-C@W systems.

The dependence of carbon structure evolution including sp , sp^2 and sp^3 hybridizations on the temperature increased from 300 to 1500 K is shown in Figure 2 (see Figure S2 for the

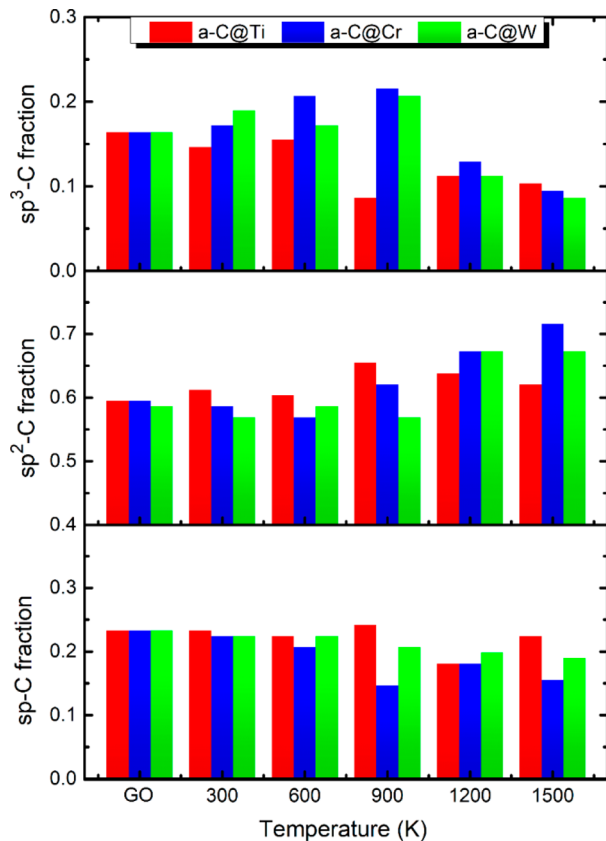


Figure 2. Evolution of hybridized carbon structure (sp , sp^2 , and sp^3) with the increase in temperature from 300 to 1500 K in the a-C@Ti, a-C@Cr, and a-C@W systems. The case after GO is also considered for comparison.

corresponding configurations of coordinated carbon structure at different temperature). Noted that different transition layers show different effect on the change of a-C structure. In a-C@Ti system, the $\text{sp}^2\text{-C}$ fraction in a-C structure with increasing the temperature from GO to 900 K increases gradually, and then decreases with further increasing the temperature to 1500 K, which shows the contrary dependence of $\text{sp}^3\text{-C}$ fraction on temperature; the maximal $\text{sp}^2\text{-C}$ fraction of 66 at. % is obtained at 900 K. However, in both the a-C@Cr and a-C@W systems, the change of $\text{sp}^2\text{-C}$ fraction with temperature reveals the opposite tendency to that of the a-C@Ti case, which decreases slightly first and then increases significantly. This trend is consistent with the $\text{sp}^3\text{-C}$ fraction, but is also contrary to the change of $\text{sp}^3\text{-C}$ fraction; when the temperature is 1500 K, the $\text{sp}^2\text{-C}$ fractions in a-C@Cr and a-C@W systems reach to 72 at. % and 67 at. %, respectively. Therefore, it indicates that at the

lower temperature (< 900 K), the Ti illustrates better catalyzed effect on a-C structure than Cr or W cases, while at the higher temperature (> 900 K), the Cr- or W-catalyzed transformation from a-C to graphitization structure is more obvious.

Figure 3 shows the further structure analysis for the temperature-dependent $\text{sp}^2\text{-C}$ structure in each system, and the number of five-, six-, and seven-membered rings only from $\text{sp}^2\text{-C}$ structures is also given representatively. In a-C@Ti system, the number of seven-membered ring decreases gradually, whereas the number of five- and six-membered rings increases first from 300 to 900 K and then decreases with further increasing to 1500 K; when the temperature is 900 K, the maximal polygonal ring number is obtained. In the a-C@Cr system, the number of five- and six-membered rings increases monotonically with increasing temperature from 300 to 1500 K; the maximal polygonal ring number is achieved at the temperature of 1500 K for this case. The evolution of polygonal rings with temperature in a-C@W system is similar to that in a-C@Cr case.

In a-C@Ti system, the $\text{sp}^3\text{-C}$ atoms are quickly converted to $\text{sp}^2\text{-C}$ atoms at the lower temperature ($T < 900$ K), which leads to the higher $\text{sp}^2\text{-C}$ fraction and the number of polygonal rings, accounting for the experimental result;¹⁰ with further increase of temperature from 900 to 1500 K, the number of isolated C atoms increases and more C atoms diffuse into Ti layers (Figure 1c) to form the stable covalent bond.²⁰ This redissolving behavior of the grown graphitic structures induced by Ti results in the reduction of $\text{sp}^2\text{-C}$ fraction and polygonal rings, as can be seen from Figures 2 and 3. But in a-C@Cr systems, a few of unstable $\text{sp}\text{-C}$ structures tend to interact with the neighbored $\text{sp}^2\text{-C}$ atoms (Figure 2), causing the slight decreased $\text{sp}^2\text{-C}$ fraction at lower temperature ($T < 600$ K); as increasing the temperature to 1500 K, the $\text{sp}^3\text{-C}$ transforms into $\text{sp}^2\text{-C}$ quickly, and there is no reverse dissolution of grown graphitic structures into Cr layers observed (Figure 1c), which is the reason for the fast increase of $\text{sp}^2\text{-C}$ fraction (Figure 2) and polygonal rings (Figure 3). The system with W atoms shows the similar behavior for the graphitic transformation of amorphous structures to that in a-C@Cr system. The calculation results are consistent with our preliminary experimental study in Figure S3, where the similar carbon roll structure changes and graphitic transformation are achieved. In addition, previous study revealed that Ti with four valence electrons tended to interact with C atom in the form of bonding state, whereas Cr or W bonded the weaker nonbonding state with C atom, respectively.²⁰ Thus the weak stability of Cr-C or W-C bonds also contribute to the obvious catalytic behavior of carbon structure at high temperature.

In conclusion, we performed the AIMD simulations to comparatively investigate the effect of Ti, Cr, or W transition layers on a-C structure evolution with temperature ranged from 300 to 1500 K. Our simulation suggested that for each case, the carbon roll structure was generated. Specifically, Ti layers showed stronger catalyzed effect on the graphitic transformation of amorphous carbon structures at lower temperature ($T < 900$ K) than Cr or W layers, whereas the evolution of a-C to graphitization induced by Cr or W layers is more obvious at the higher temperature ($T > 900$ K). This result not only provides the guidance for the design and selection of a-C film with transition layers for wide industrial application, but also offers a facile strategy to fabricate the special functionalized carbon structure from large area a-C film catalyzed by metallic layers.

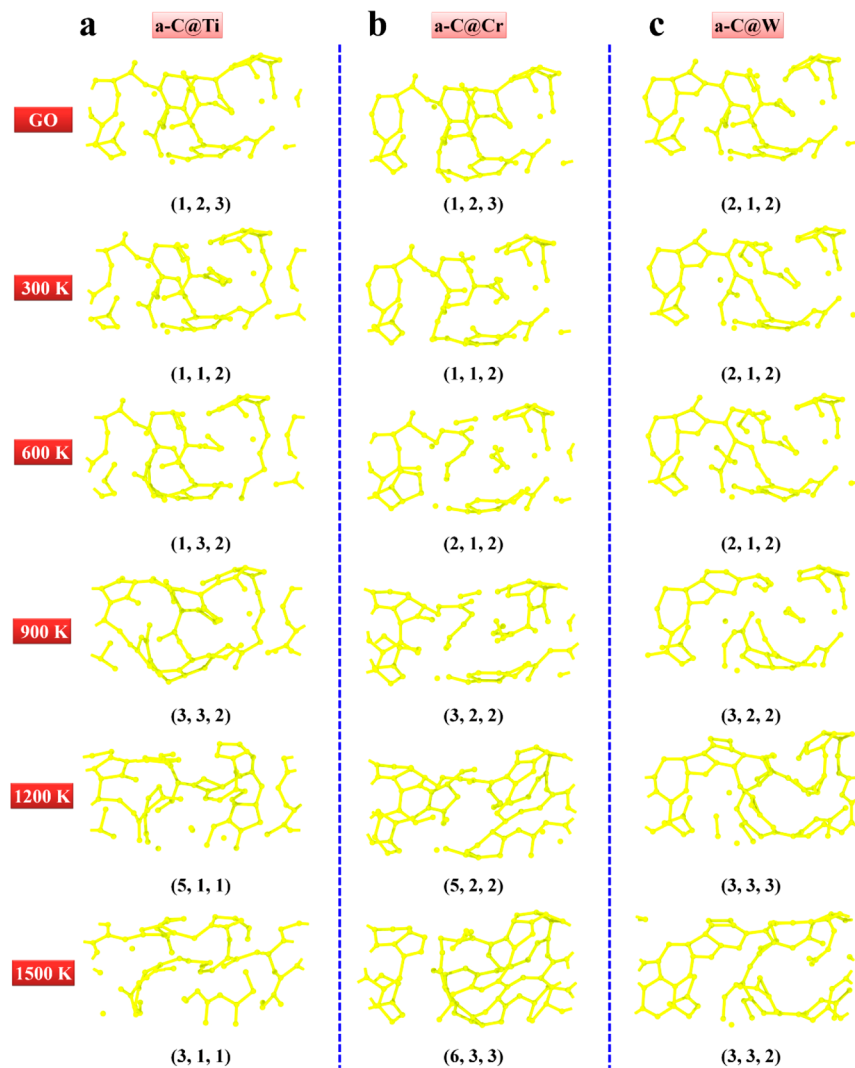


Figure 3. Temperature-dependent sp^2 -C structure evolution of (a) a-C@Ti, (b) a-C@Cr, and (c) a-C@W based on AIMD simulations with the increase in temperature from 300 to 1500 K. The numbers in brackets below the C structures indicate the number of five, six, and seven-membered rings within the sp^2 -C network. The Ti, Cr, or W layers and the C atoms with coordination number of 0, 1, 2, and 4 are omitted to highlight the change of only sp^2 -C structures.

ASSOCIATED CONTENT

Supporting Information

The Supporting Information is available free of charge on the ACS Publications website at DOI: [10.1021/acsami.7b12179](https://doi.org/10.1021/acsami.7b12179).

Energy change during the relaxation at each temperature in a-C@Ti, a-C@Cr, and a-C@W systems; temperature-dependent coordinated C structure evolution for each case; and the preliminary experimental result of a-C film with Cr transition layers ([PDF](#))

AUTHOR INFORMATION

Corresponding Authors

*E-mail: lxw0826@gmail.com. Tel: 82-2-958-5450. Fax: 82-2-958-5451 (X.L.).

*E-mail: aywang@nimte.ac.cn. Tel: 86-574-86685170. Fax: 86-574-86685159 (A.W.).

ORCID

Xiaowei Li: [0000-0002-7042-2546](https://orcid.org/0000-0002-7042-2546)

Notes

The authors declare no competing financial interest.

ACKNOWLEDGMENTS

This research was supported by the National Key R&D Program of China (2017YFB0702303), National Natural Science Foundation of China (51772307), the Korea Research Fellowship Program through the National Research Foundation of Korea (NRF) funded by the Ministry of Science and ICT (No 2017H1D3A1A01055070), and the Nano Materials Research Program through the Ministry of Science and IT Technology (2NS1480). We thank Dr. Kwang-Ryeol Lee from Korea Institute of Science and Technology for providing research platform and helpful discussion.

REFERENCES

- (1) Robertson, J. Diamond-Like Amorphous Carbon. *Mater. Sci. Eng., R* **2002**, *37*, 129–281.
- (2) Zhang, L.; Wei, X.; Lin, Y.; Wang, F. A Ternary Phase Diagram for Amorphous Carbon. *Carbon* **2015**, *94*, 202–213.
- (3) Huang, J.; Wang, L.; Liu, B.; Wan, S.; Xue, Q. Vitro Evaluation of the Tribological Response of Mo-Doped Graphite-Like Carbon Film in Different Biological Media. *ACS Appl. Mater. Interfaces* **2015**, *7*, 2772–2783.

- (4) Bewilogua, K.; Hofmann, D. History of Diamond-Like Carbon Films – From First Experiments to Worldwide Applications. *Surf. Coat. Technol.* **2014**, *242*, 214–225.
- (5) Chopra, K. L.; Paulson, P. D.; Dutta, V. Thin-Film Solar Cells: an Overview. *Prog. Prog. Photovoltaics* **2004**, *12*, 69–92.
- (6) Veerappan, G.; Bojan, K.; Rhee, S. W. Amorphous Carbon as a Flexible Counter Electrode for Low Cost and Efficient Dye Sensitized Solar Cell. *Renewable Energy* **2012**, *41*, 383–388.
- (7) Yi, P.; Peng, L.; Feng, L.; Gan, P.; Lai, X. Performance of a Proton Exchange Membrane Fuel Cell Stack Using Conductive Amorphous Carbon-Coated 304 Stainless Steel Bipolar Plates. *J. Power Sources* **2010**, *195* (20), 7061–7066.
- (8) Chen, X.; Peng, Z.; Fu, Z.; Yue, W.; Yu, X.; Wang, C. Influence of Individual C-C Layer Thickness on Structure and Tribological Properties of Multilayered Cr-C/a-C: Cr Thin Films. *Surf. Coat. Technol.* **2010**, *204* (20), 3319–3325.
- (9) Li, Y. S.; Tang, Y.; Yang, Q.; Xiao, C.; Hirose, A. Growth and Adhesion Failure of Diamond Thin Films Deposited on Stainless Steel with Ultra-Thin Dual Metal Interlayers. *Appl. Surf. Sci.* **2010**, *256* (24), 7653–7657.
- (10) Lee, K. M.; Han, H. J.; Choi, S.; Park, K. H.; Oh, S.; Lee, S.; Koh, K. H. Effects of Metal Buffer Layers on the Hot Filament Chemical Vapor Deposition of Nanostructured Carbon Films. *J. Vac. Sci. Technol., B: Microelectron. Process. Phenom.* **2003**, *21* (1), 623–626.
- (11) Xiong, W.; Zhou, Y. S.; Jiang, L. J.; Sarkar, A.; Mahjouri-Samani, M.; Xie, Z. Q.; Gao, Y.; Ianno, N. J.; Jiang, L.; Lu, Y. F. Single-Step Formation of Graphene on Dielectric Surface. *Adv. Mater.* **2013**, *25*, 630–634.
- (12) Wu, Z.; Guo, Y.; Guo, Y.; Huang, R.; Xu, S.; Song, J.; Lu, H.; Lin, Z.; Han, Y.; Li, H.; Han, T.; Lin, J.; Wu, Y.; Long, G.; Cai, Y.; Cheng, C.; Su, D.; Robertson, J.; Wang, N. A Fast Transfer-Free Synthesis of High-Quality Monolayer Graphene on Insulating Substrates by a Simple Rapid Thermal Treatment. *Nanoscale* **2016**, *8*, 2594–2600.
- (13) Li, X.; Guo, P.; Sun, L.; Wang, A.; Ke, P. Ab Initio Investigation on Cu/C Codoped Amorphous Carbon Nanocomposite Films with Giant Residual Stress Reduction. *ACS Appl. Mater. Interfaces* **2015**, *7*, 27878–27884.
- (14) Kresse, G.; Furthmüller, J. Efficiency of Ab Initio Total Energy Calculations for Metals and Semiconductors Using Plane-Wave Basis Set. *Comput. Mater. Sci.* **1996**, *6*, 15–50.
- (15) Kresse, G.; Furthmüller, J. Efficient Iterative Schemes for Ab Initio Total-Energy Calculations Using a Plane-Wave Basis Set. *Phys. Rev. B: Condens. Matter Mater. Phys.* **1996**, *54*, 11169–11186.
- (16) Perdew, J. P.; Burke, K.; Ernzerhof, M. Generalized Gradient Approximation Made Simple. *Phys. Rev. Lett.* **1996**, *77*, 3865–3868.
- (17) Gillan, M. J. Calculation of the Vacancy Formation Energy in Aluminum. *J. Phys.: Condens. Matter* **1989**, *1*, 689–711.
- (18) Chen, S.; Xiong, W.; Zhou, Y. S.; Lu, Y. F.; Zeng, X. C. An Ab Initio Study of the Nickel-Catalyzed Transformation of Amorphous Carbon into Graphene in Rapid Thermal Processing. *Nanoscale* **2016**, *8*, 9746–9755.
- (19) Li, X.; Ke, P.; Wang, A. Probing the Stress Reduction Mechanism of Diamond-Like Carbon Films by Incorporating Ti, Cr, or W Carbide-Forming Metals: Ab Initio Molecular Dynamics Simulation. *J. Phys. Chem. C* **2015**, *119* (11), 6086–6093.
- (20) Li, X.; Zhang, D.; Lee, K. R.; Wang, A. Effect of Metal Doping on Structural Characteristics of Amorphous Carbon System: A First-Principles Study. *Thin Solid Films* **2016**, *607*, 67–72.